Design Feasibility of a Vortex Induced Vibration Based Hydro-Kinetic Energy Harvesting System

Conference Paper · May 2011

DOI: 10.1109/GREEN.2011.5754879 · Source: IEEE Xplore

4 authors, including:

Arindam Banerjee
Lehigh University
75 PUBLICATIONS **866** CITATIONS

SEE PROFILE

J.W. Kimball
Missouri University of Science and Technology
131 PUBLICATIONS **3,489** CITATIONS

SEE PROFILE

Design Feasibility of a Vortex Induced Vibration Based Hydro-Kinetic Energy Harvesting System

Varun Lobo[1], Nyuykighan Mainsah[2], Arindam Banerjee[1] and Jonathan W. Kimball[2,3]
[1]Department of Mechanical and Aerospace Engineering
[2]Department of Electrical and Computer Engineering
Missouri University of Science and Technology, Rolla 65409, Missouri, USA
[3]E-mail: kimballjw@mst.edu

***Abstract*- The vortex induced vibration (VIV) based power generating system discussed in this paper is a new concept in power generation from fluid flows in oceans, rivers and streams. The possibility of harnessing energy from the vibrations incurred in a bluff body due to the phenomenon known as VIV, in which motion is induced on a body facing an external flow due to the periodic irregularities in the flow caused by boundary layer separation is explored. The VIV system is based on the idea of maximizing rather than spoiling vortex shedding and exploiting rather than suppressing VIV. The vibrating bodies are in turn used to harness energy using an efficient power-take-off system. The study of fluid dynamics, along with maintaining vortex shedding over the synchronization range, plays an important role in the design of such a system. Apart from this, the main challenge in the design of a VIV generator is introducing optimal damping and low mass ratios for high energy conversion and an efficient power take-off mechanism. This work presents a scoping study of such a device. In contrast to previous work on forced vibrations, the present study focuses on free vibrations that arise due to the shedding of vortices from a cylinder. The working and design considerations of the energy converter is outlined starting with a set of basic definitions pertaining to this technology.**

***Keywords*-** *Vortex induced vibration, vortex shedding, boundary layer separation.*

Nomenclature:

u	velocity of free stream
ν	kinematic viscosity
L	length of cylinder
D	cylinder diameter
f_n	natural frequency of the system
f	vortex shedding frequency
m	oscillating mass includes effective mass of the spring
m_a	effective mass of spring
A	amplitude of vibration
C_A	ideal mass added (= 1.0 for a cylinder)
C	coefficient of damping
k	*Spring constant*
F_{peak}	peak force
P_{avg}	average power

Non-Dimensional Parameters:

m^* (mass ratio) = $4m/\rho\pi D^2 L$

A^* (amplitude ratio) = A/D

ζ (damping ratio) = $c/\sqrt{k(m+m_a)}$

U^* (velocity ratio) = $u/f_n D$

f^* (frequency ratio) = f/f_n

Re (Reynolds number) = uD/ν

I. INTRODUCTION

Due to the rapid depletion of fossil fuel reserves, alternate and sustainable energy resources are being sought in order to maintain the growing global energy requirements. Some of the well researched alternative sources include bio-fuels, solar, wind, hydro and geo-thermal energy. Hydrokinetic energy from flow of rivers, streams and artificial water channels are considered to be a viable resource [2, 3].

This paper focuses on a VIV based system for the extraction of hydrokinetic energy. When compared to other alternative resources such as wind or solar, the VIV generator is considered more economically viable (i.e. low cost of generated power in terms of $/kWh - see Figure 1) mostly due to its simple and robust design (Figure 2). Figure 1 compares our VIV system with other alternative energy sources using benchmarking data from [1]. In this manuscript, we focus on the use of computational fluid dynamics (CFD) to discuss the VIV generator's optimal geometric characteristics. The operating conditions of a new free-vibration-based VIV generator is determined through CFD analysis for various design parameters, which include the aspect ratio (L/d), mass ratio (m^*), spring constant (k), damping coefficient (c) and damping ratio (ζ). A preliminary design of a linear generator and accompanying power converter is also discussed.

The current system is similar in design to the VIVACE

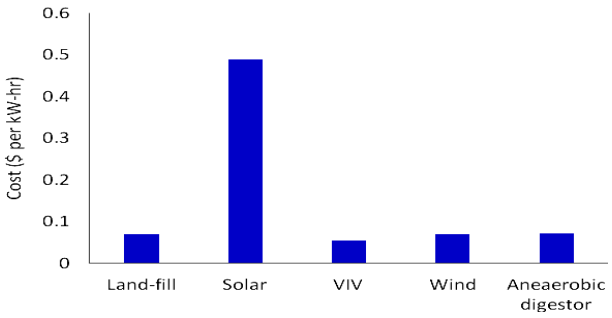

Figure 1. Cost comparison between alternate sources of power and vortex based energy source [1].

(VIV-aquatic clean energy) generator invented by Bernitsas and Raghavan and patented through the University of Michigan [4-6]. The VIVACE generates electrical energy utilizing *forced vibration* of oscillating cylinders in a given fluid flow. However, our system focuses entirely on *free vibrations* rather than forced vibrations of a cylinder caused due to the shedding of vortices from its surface.

II. Principles and Design of a VIV Generator

VIV of structures is important to many fields of engineering. Vibrations due to vortex shedding from the surface of a body can cause damage to mechanical, civil, aerospace, marine & offshore structures. It causes vibrations in many structures such as buildings and bridges, riser tubes bringing oil from the sea bed to the surface and bundle tubes in a heat exchanger. The importance of VIV has led to a large number of fundamental studies [7-9]. Various numerical simulations [10, 11] and experiments [12] have also been performed to better understand VIV. Figure 2 presents a basic schematic of the VIV generator system for a single cylinder that is coupled with a spring and a damper attached to it. The VIV generator discussed in this paper contains a rigid cylinder in a fluid flow that is mounted elastically using a spring-damping system along with an effective power take off mechanism (damper) attached to it.

The cylinder in our system is constrained to move only in the vertical y-direction. As separation of the boundary layer begins to take place on the surface of the body, a pressure variation results along the circumference of the cylinder, which causes the cylinder to oscillate. This separation of the boundary layer from the surface causes vortex formation in the wake region of the cylinder. The transverse oscillation of the vibrating cylinder depends upon the strength of the vortex formed. As the Reynolds number increases due to an increase in the flow velocity, lock in or vortex synchronization takes place. The phenomenon of lock-in or synchronization [13] suggest that as the fluid velocity increases, a speed is reached when the ratio of vortex shedding frequency to the natural frequency becomes close to unity [14].

The amplitude of vibrations in VIV is another important design parameter for building an efficient VIV generator. There exists two types of response modes in any system depending upon the mass-damping parameter [15, 16]. For a high mass-damping parameter, an initial and lower amplitude branch is present [16]. However in the case of a low mass-damping system there exists a higher amplitude branch called the upper branch [17]. This is shown in Figure 3 below. Feng performed experiments in a wind tunnel which resulted in a higher mass ratio (m^*) [16]. Khalak and Williamson [18] also performed similar experiments using water as their working fluid and came across a third response branch called the "upper branch." Thus, it is evident from the above two classical experiments that for maximum amplitude it is necessary for the system to have low mass and damping. Experiments performed by Govardhan and Williamson [19] has proved the existence of critical mass ratio (m^*) to be equal to 0.54. Since our system is designed for cylinders with very low mass (for which mass ratios (m^*) $\leq$ 0.54), the corresponding lower branch frequency given by [19]

$$f^*_{lower} = \sqrt{(m^* + 1)/(m^* - 0.54)} \qquad (1)$$

does not exist as seen in Figure 4. Hence the system exists in the upper branch only with maximum vibrations.

Every vortex formed in the wake region of an object comprises of either a single vortex (*S*) or pair of vortices (*P*) giving patterns such as 2*S*, 2*P*, and *P*+*S* modes, which are the principle modes in the fundamental lock-in region. Brika and Laneville [20] were the first to show the presence of *2P* mode in free vibrations with clear correspondence of the *2S* mode being associated with the lower branch while the *2P* mode was associated with the upper branch. Other patterns like the *2P*+*2S* and the *P*+*S* are formed due to the coalescence of one or more vortices. The significance of these modes from controlled vibrations is that they provide a map of regimes within which we observe certain branches of free vibrations.

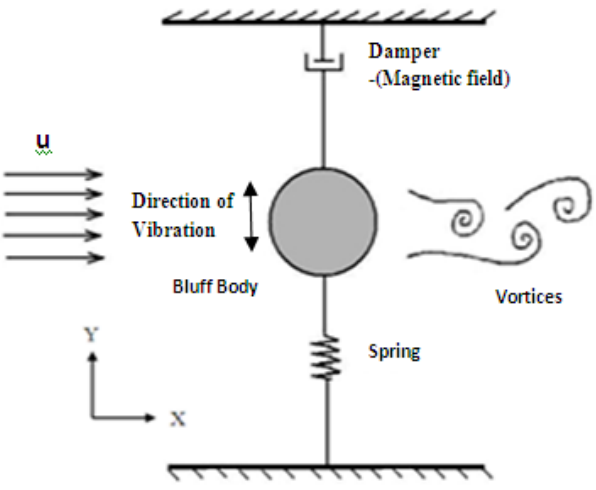

Figure 2. A schematic diagram of a VIV generator module for a single cylinder system.

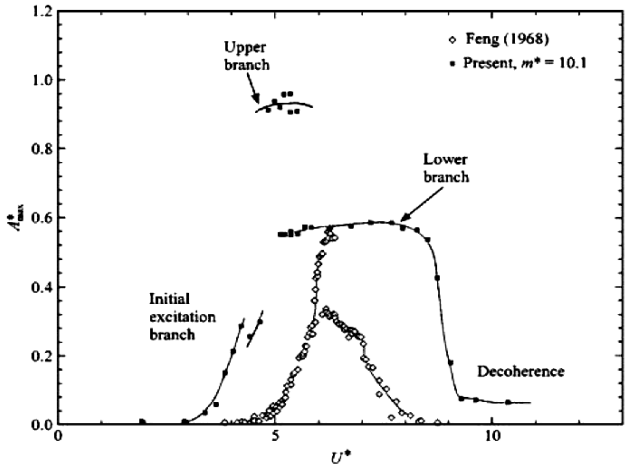

Figure 3. Synchronization regime of high amplitude vibration extends to infinite velocities as m* approached the value of 0.54 [12]

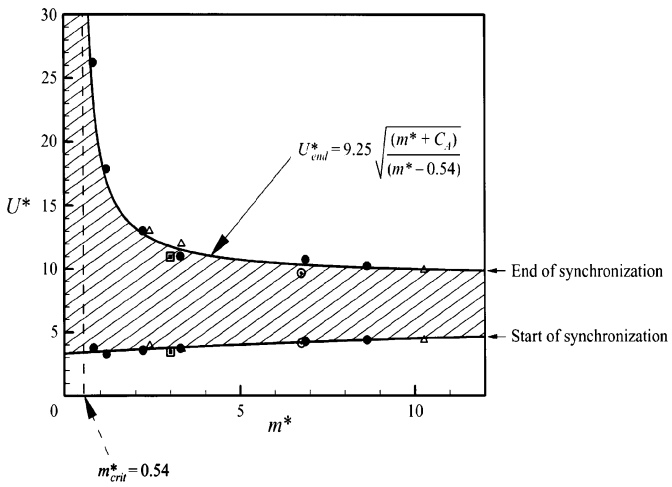

Figure 4. Comparison of Feng's [16] maximum A/D with those obtained by Khalak and Williamson [18].

The design parameters for our CFD simulation based design are selected such that m* is always below $m^*_{critical}$. Table 1 lists the various parameters for the design cases we present in this manuscript. The average power and the peak force acting on the cylinder for maximum amplitude to diameter ratio are also shown. The peak force (2) and the average power (3) are given by the following expressions.

$$F_{peak} = A \times \pi \times f_n \times C \tag{2}$$

$$P_{avg} = F^2_{peak} \big/ 2C \tag{3}$$

From (2)-(3), we observe that the peak force and the average power distribution is a direct function of the coefficient of damping, amplitude and the frequency of the system. The greater the coefficient of damping, the lesser the maximum amplitude attained but greater power is harnessed provided the damping is due to the power-take-off system. Power and force on the cylinder is also a function of the amplitude attained which can be seen by comparing case 6 and 7. Thus factors like damping coefficient, Reynolds number, mass ratio etc play a very important role in power extraction.

III. Numerical Method

The system design analysis was performed using ANSYS-CFX, SolidWorks, and ANSYS ICEM meshing software to model the fluid flow and monitor vortex formations. ANSYS-CFX is control-volume-based commercial CFD software used to solve the conservation equations of mass and momentum governing fluid dynamics. Since the motion of the cylinder is being actuated by fluid flow, the simulation involves non-linear fluid structure interaction (FSI) and subsequent mesh motion. The mesh that was used for this simulation is a structured hexa mesh [21]. The quality of mesh, such as the element skewness, expansion ratio, minimum orthogonal angle and aspect ratio, were monitored to maintain mesh quality. For the FSI to take place, a CFX Expression Language (CEL) code was developed in CFX-ANSYS. It consisted of physical properties of the cylinder, transient state definitions and governing equations that couple together the fluid forces and cylinder displacements. The CEL code was developed using the governing equation describing the motion of a vibrating rigid body:

TABLE 1: VIV GENERATOR MODEL PARTICULARS

Case	1	2	3	4	5	6	7	8
Dia(m)	0.08	0.08	0.08	0.08	0.08	0.08	0.05	0.05
K	15	15	50	25	15	15	15	15
C	2.6	2.6	2.6	2.6	25	5	2.6	2.6
Re	8×10^4	4×10^4	8×10^4	8×10^4	8×10^4	8×10^4	5×10^4	1×10^5
m^*	0.315	0.315	0.315	0.315	0.315	0.315	0.5	0.5

$$m\ddot{y} + c\dot{y} + ky = F(t) \tag{4}$$

with $F(t)$ being the hydrodynamic force, $m\ddot{y}$ being the body force, $c\dot{y}$ the damping force and ky the spring force acting on the surface of the rigid body. For small oscillations at the synchronous range, a good approximation of the transverse force is given by a sinusoid at the vortex shedding frequency:

$$F(t) = F\sin(\omega t + \varphi) \tag{5}$$

where F is the force acting on the cylinder due to the vortex shedding from the surface also known as the hydrodynamic force and φ is the phase angle between the fluid force and body displacement. Both of these components are crucial in determining the energy transfer from the working fluid to the surface of the body and thus influence the amplitude of oscillation [7, 22].

According to the characteristics of the boundary layer shear separation over the cylinder surface, Zdravkovich [23] subdivided the flow over a smooth cylinder into 15 characteristic regimes. Based on this classification, the ranges of Reynolds number in which our simulations were performed belongs to the TrSL2 subcritical regime where $2 \times 10^3 \langle Re \langle 1 \times 10^5$. To account for this range of Reynolds number (see Table 1) of the flow, *k*-ω turbulence model [24] (8)-(9) has been used, where ρ is the density, μ is the turbulent viscosity, P_k is the production rate of turbulence, k is the specific turbulence kinetic energy and ω is the dissipation per unit turbulent kinetic energy. As there is no molecular diffusion term, this model applies strictly to high Reynolds number flows. The *k*-ω model does not involve the complex non-linear viscous damping function as used in the *k*-ε model and is therefore more accurate and robust, thus making it ideal for these types of flows.

The basic governing equations that were used are as follows:

a) Continuity

$$\nabla \cdot \vec{V} = 0 \tag{6}$$

b) Navier-Stokes:

$$\frac{d\vec{V}}{dt} = -\frac{1}{\rho}\nabla p + \vec{g} + \frac{1}{\rho}\nabla.\vec{\tau}_{ij} \tag{7}$$

c) *k*-equation:

$$\frac{\partial(\rho k)}{\partial(t)}+\nabla\cdot(\rho U k)=\nabla\cdot\left[\left(\mu+\frac{\mu_t}{\sigma_k}\right)\nabla k\right]+P_k-\beta'\rho k\omega \quad (8)$$

d) ω-equation:

$$\frac{\partial(\rho\omega)}{\partial(t)}+\nabla\cdot(\rho U\omega)=\nabla\cdot\left[\left(\mu+\frac{\mu_t}{\sigma_\omega}\right)\nabla\omega\right]+\alpha\frac{\omega}{k}P_k-\beta'\rho\omega^2 \quad (9)$$

Convergence criteria have been set such that the residuals for the continuity, *x*-momentum, *y*-momentum, *z*-momentum, k and ω are less than 10^{-4}.

IV. Results from CFD Design Calculations

Table 2 presents a brief summary of the energy extraction from a single cylinder VIV system. It should be noted that the present system is conservative in nature and has not been optimized yet. The peak force listed in Table 2 is the maximum force that can be extracted from our VIV system having the specifications listed in Table 1. The mass ratio in all the four cases was kept below the critical mass ratio of 0.54 for obtaining the maximum amplitude. All the simulations are 3-D and based on an L/d ratio of 1 to reduce computational costs. The amount of damping that is provided to the system is directly proportional to the power generated, provided the damping is due to the power take off system and other damping sources like structural and system damping is negligible. Comparing cases 1 and 2 and 7 and 8, it is seen that as the Reynolds number decreases, the displacement and thus the peak force decreases. Higher Reynolds number imparts greater force on the surface thus increasing power output. Case 1, 5 and 6 show that as the damping coefficient increases, the maximum displacement decreases. From case 1 and 7, the effect of change in diameter is clearly evident. Thus increasing the diameter imparts greater force on the cylinder and thus greater displacement and power output.

V. Power Take-Off

The above discussion concerned the fluid dynamics that give rise to vibrations. To make this system an effective energy harvester, a mechanism is needed to convert these vibrations to some useful form of energy. The selected architecture is a tubular linear interior permanent magnet generator (TL-IPM) [25] connected to a power converter as shown in Figure 5. A linear generator was chosen to minimize mechanical components, such as gears or cams. A linear generator has two main portions: a stator and a translator (also called slider or mover). The translator takes the place of the rotor in a conventional rotating machine and houses the permanent magnets. The translator could either occupy the inner or outer diameter of the tubular structure. For our application, the translator occupies the inner section and stator the outer diameter. Figure 6 shows the planned TL-IPM.

There are two topologies of linear generator design, long translator type and long stator types [26]. Following the notation of [25], a Θ type machine has a long stator that completely encloses the translator and a Ξ type machine has a long translator that exits the stator. Given the relatively slow motion of the translator, a better performance (high power density, high efficiency) configuration is preferred. From the efficiency of the machine point of view, the long translator would be the better choice. However, there is a severe mass constraint for the moving portion in the VIV system, so we have chosen the Θ (short translator, long stator) configuration.

The coil windings within the stator are supported by sleeves or placed inside slots. Hence, the other 2 variants of the linear generator include an air-cored stator (slotless) and an iron-cored stator (slotted) [27]. Each variant comes with its advantages and drawbacks. The magnetic field produced by the PMs results in significant attraction between the translator and stator which must be withstood by the mechanical tubular structure [28] of the take-off system. Significant structural savings can be made if these cogging forces can be reduced or eliminated, which can be achieved by having a stator which contains no iron (air-cored), which is a simpler and cheaper

TABLE 2. ESTIMATION OF THE UPPER LIMIT OF VIV CONVERSION.

Case	1	2	3	4	5	6	7	8
A/D	0.325	0.1312	0.175	0.262	0.178	0.212	0.2	0.5
F_{peak} (N)	0.75	0.152	0.4	0.61	1.678	0.9346	0.5015	2.5
P_{avg} (W)	0.1	0.004	0.03	0.07	0.056	0.087	0.047	1.1

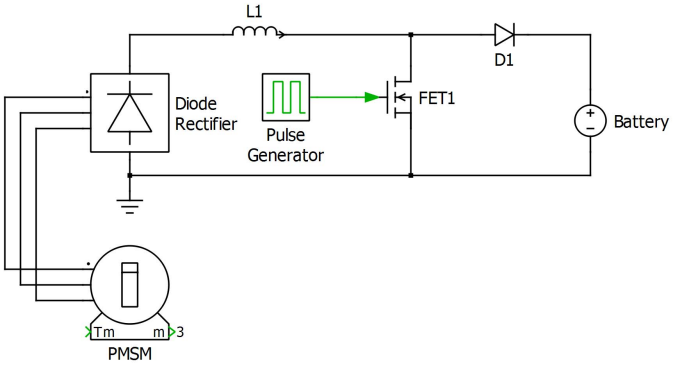

Figure 5. Simplified schematic for energy harvesting.

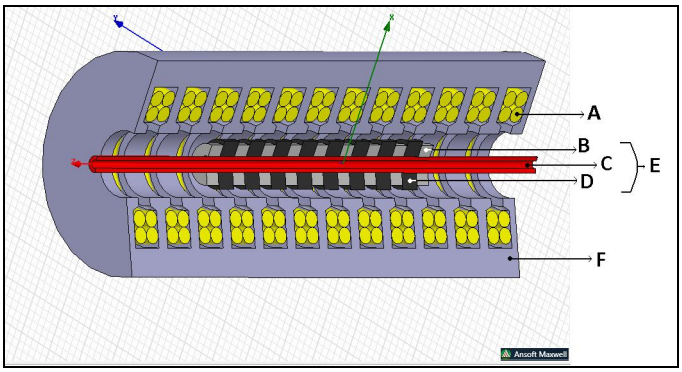

Figure 6. Proposed TL-IPM. Parts: A. Coil Windings; B. Ferromagnetic Material (e.g. Iron); C. Support Tube; D. Permanent Magnet; E. Translator; F. Stator

construction option. In the iron-cored stator, magnetic flux generated by the PMs in translator is more concentrated inside the windings. This results in a significantly higher field density resulting in a higher induced voltage per translator stroke compared to the air-cored configuration [27]. Again, because the mass of the translator (and therefore the available magnetic material) is severely constrained, the slotted variant has been chosen.

The main flux direction in the translator is determined by the magnetization of the PMs. With both radial and axial magnetization, ferromagnetic materials are generally required to guide the desired flux paths [29]. Both have been found to produce harmonic content, with the axially-aligned buried magnets producing very low harmonic content with suitable flux levels and radially-aligned buried magnets having slightly more harmonics [30]. To minimize harmonics and cogging forces, the proposed design uses axially-aligned buried magnets, as shown in Figure 7. We have chosen neodymium-iron-boron (NdFeB) magnets because of their high remanence and coercivity.

Figure 8 is a dimensioned drawing of the proposed TL-IPM. Parameters are given in Table 3. This design was driven by two main considerations: force vs. displacement and translator mass. Following the methodology of [25], the peak force is estimated at 1.04 N with a translator mass of 22.8 g. This is greater than half the desired force with less than half the desired translator mass, so that two generators may be connected to each cylinder (one at each end).

Figure 5 above contains the proposed power converter. The boost converter is controlled as in a power factor correction circuit. The current is proportional to the rectified voltage, and the proportionality constant (conductance, G=1/R) determines the effective damping that the machine provides. This is conceptually similar to the resistor emulation approaches in [31, 32]. As shown in [32], the emulated resistance R_{em} of a boost converter in discontinuous conduction mode is

$$R_{em} = \frac{2LT}{t_{on}^2}\left(\frac{V_{out} - V_{in}}{V_{out}}\right) \tag{10}$$

where L is the inductance, T is the switching period, t_{on} is the on-time of the controlled switch, and V_{out} and V_{in} are the output and input voltages, respectively. The input power is then V_{in}^2 / R_{em}, which is equivalent to a damper in the mechanical system.

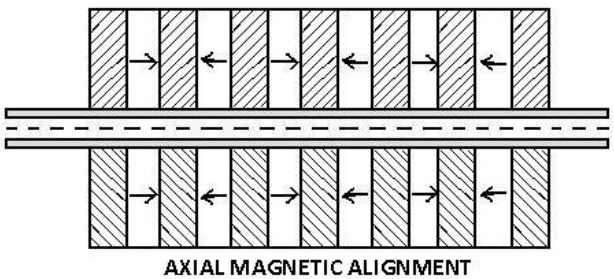

Figure 7. Translator with axial magnetic alignment, indicating magnet polarities.

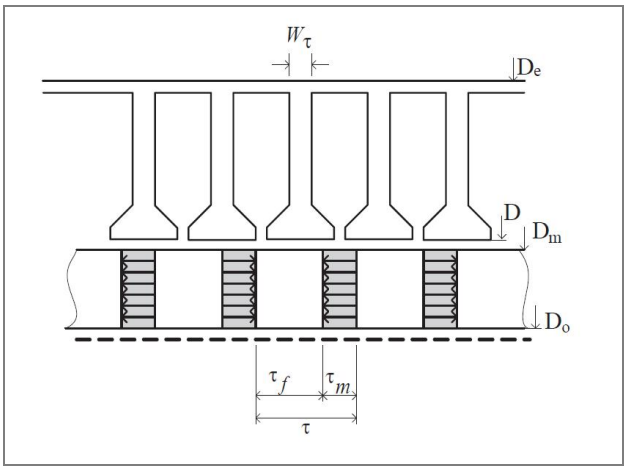

Figure 8. Dimensioned drawing of TL-IPM (adapted from [25]).

TABLE 3. DIMENSIONS FOR FIGURE 8.

Parameter	Dimension [mm]
τ_m	3.20
τ_f	1.37
τ	4.57
D_m - D_o	9.52
W_τ	2.00
D - D_m	0.50
D_e - D	25.0
Pole Pairs	2

The optimal value of R_{em} is unknown a priori. A maximum power point tracking technique, as used for solar power [33], will be used to determine the optimal R_{em}. The most promising approach is perturb & observe.

VI. CONCLUSION AND FUTURE DIRECTIONS

This paper presents a system capable of effectively capturing the hydrokinetic energy from a fluid flowing over a bluff body causing its vibration due to the phenomenon of VIV. An energy convertor based on such working principle looks promising in the near future.

As the presence of wall or the proximity of the cylinders to the surface plays an important role in amplitude response of the cylinder, the presence of one body in the wake of another body can have considerable change in the flow pattern and hence alter forces acting on the bodies [11]. Both the flow field and force coefficients depend highly on the arrangement and spacing between bluff bodies primarily due to the wake and proximity-induced interference effects [34]. Future studies will include study of cylinder arrays in such a manner that the vortex formed due to one cylinder will only enhance the forces acting on the other cylinders present in its wake, making possible the presence of multiple cylinders in a module. In addition, we plan to study the effect of surface roughness and cylinder rotation on vortex formation and its separation from the surface in a small scale laboratory based system in the Missouri S&T water-tunnel facility.

ACKNOWLEDGMENT

The authors would like to thank Prof. Mariesa Crow for providing us with a seed grant from the Energy Research and Development Center at Missouri S&T.

REFERENCES

[1] M. M. Bernitsas, K. Raghavan, Y. Ben-Simon, and E. M. H. Garcia, "VIVACE (Vortex Induced Vibration for Aquatic Clean Energy): A new concept in generation of clean and renewable energy from fluid flow," in *Proc. 25th Intl. Conf. Offshore Mechanics and Arctic Engineering (OMAE)*, 2006, OMAE06-92645.

[2] "Proceedings of the Hydrokinetic and Wave Energy Technologies: Technical and Environment Issues Workshop," U.S Department of Energy, 2006.

[3] M. T. Pontes and A. Falcao, "Ocean Energies: Resources and Utilization," *Proceedings of 18th WEC Congress*, Oct. 2001.

[4] M. M. Bernitsas and K. Raghavan, "Converter of Current/Tide/Wave Energy," U.S. Patent Serial No. 60/628, 525, 2004.

[5] M. M. Bernitsas and K. Raghavan, "Supplement to the U.S Provisional Patent Application titled 'Converter of Current, Tide, or Wave Energy'," U.S. Patent 2005.

[6] M. M. Bernitsas and K. Raghavan, "Fluid Motion Energy Converter," U.S. Patent Serial No. 11/272,504., 2005.

[7] T. Sarpkaya, "Vortex-Induced Oscillations: A Selective Review," *Journal of Applied Mechanics*, vol. 46, pp. 241-258, 1979.

[8] R. A. Skop and O. M. Griffin, "A model for the vortex-excited resonant response of bluff cylinders," *Journal of Sound and Vibration*, vol. 27, pp. 225-233, 1973.

[9] C. H. K. Williamson and R. Govardhan, "Vortex-induced vibrations," *Annual Review of Fluid Mechanics*, vol. 36, pp. 413-455, January 2004.

[10] H. M. Blackburn and R. D. Henderson, "A study of two-dimensional flow past an oscillating cylinder," *Journal of Fluid Mechanics*, vol. 385, pp. 255-286, 1999.

[11] J. R. Meneghini and P. W. Bearman, "Numerical Simulation of High Amplitude Oscillatory Flow About a Circular Cylinder," *Journal of Fluids and Structures*, vol. 9, pp. 435-455, 1995.

[12] R. Govardhan and C. H. K. Williamson, "Modes of vortex formation and frequency response of a freely vibrating cylinder," *J. Fluid Mech.*, vol. 420, pp. 85-130, 2000.

[13] R. D. Blevins, "Flow-induced vibrations," *Journal of Sound and Vibration*, vol. 149, 1990.

[14] A. Khalak and C. H. K. Williamson, "Fluid forces and dynamics of a hydroelastic structure with very low mass and damping," *Journal of Fluids and Structures*, vol. 11, pp. 973-982, November 1997.

[15] A. Khalak and C. H. K. Williamson, "Investigation of relative effects of mass and damping in vortex-induced vibration of a circular cylinder," *Journal of Wind Engineering and Industrial Aerodynamics*, vol. 69-71, pp. 341-350, July-Oct. 1997.

[16] C. C. Feng, "The measurements of vortex-induced effects in a flow past a stationary and oscillating circular and D-section cylinders," Univ. BC, Vancouver, Can., 1968.

[17] R. Govardhan and C. H. K. Williamson, "Resonance forever: existence of a critical mass and an infinite regime of resonance in vortex-induced vibration," *Journal of Fluid Mechanics*, vol. 473, pp. 147-166, 2002.

[18] A. Khalak and C. H. K. Williamson, "Motions, forces and mode transitions in vortex-induced vibrations at low mass-damping," *Journal of Fluids and Structures*, vol. 13, pp. 813-851, October 1999.

[19] R. Govardhan and C. H. K. Williamson, "Critical mass in vortex-induced vibration of a cylinder," *European Journal of Mechanics - B/Fluids*, vol. 23, pp. 17-27, 2003.

[20] D. Brika and A. Laneville, "Vortex-induced vibrations of a long flexible circular cylinder," *Journal of Fluid Mechanics*, vol. 250, pp. 481-508, May 1993.

[21] ANSYS, "CFX 12.0.1 User's guide," ANSYS INC., 2010.

[22] P. W. Bearman, "Vortex Shedding from Oscillating Bluff Bodies," *Annual Review of Fluid Mechanics*, vol. 16, pp. 195-222, 1984.

[23] M. M. Zdravkovich, "Conceptual overview of laminar and turbulent flows past smooth and rough circular-cylinders," *Journal of wind engineering and industrial aerodynamics*, vol. 33, pp. 53-62, 1990.

[24] D. C. Wilcox, *Turbulence modeling for CFD*: DCW Industries, Inc., 1994.

[25] N. Bianchi, S. Bolognani, D. Dalla Corte, and F. Tonel, "Tubular linear permanent magnet motors: an overall comparison," *IEEE Transactions on Industry Applications*, vol. 39, pp. 466-475, Mar/Apr 2003.

[26] P. Hew Wooi, H. Arof, and Wijono, "Design of a Permanent Magnet Linear Generator," in *Proc. Strategic Technology, The 1st International Forum on*, 2006, pp. 231-234.

[27] L. Szabo, C. Oprea, l. A. Viorel, and K. A. Biro, "Novel Permanent Magnet Tubular Linear Generator for Wave Energy Converters," in *Proc. Electric Machines & Drives Conference, 2007. IEMDC '07. IEEE International*, 2007, vol. 2, pp. 983-987.

[28] N. J. Baker, M. A. Mueller, and E. Spooner, "Permanent magnet air-cored tubular linear generator for marine energy converters," in *Proc. Power Electronics, Machines and Drives, 2004. (PEMD 2004). Second International Conference on (Conf. Publ. No. 498)*, 2004, vol. 2, pp. 862-867 Vol.2.

[29] L. Cheng-Tsung and L. Hsin-Nan, "Development of a systematic scheme for direct driven slotless tubular linear generator design," in *Proc. Power Electronics and Drive Systems, 2009. PEDS 2009. International Conference on*, 2009, pp. 843-847.

[30] D. M. Joseph and W. A. Cronje, "Design and Analysis of a Double-Sided Tubular Linear Synchronous Generator with Particular Application to Wave-Energy Conversion," in *Proc. Power Engineering Society Conference and Exposition in Africa, 2007. PowerAfrica '07. IEEE*, 2007, pp. 1-8.

[31] Y. Tan and S. Panda, "Optimized Wind Energy Harvesting SystemUsing Resistance Emulator and Active Rectifierfor Wireless Sensor Nodes," *Power Electronics, IEEE Transactions on*, vol. PP, pp. 1-1.

[32] T. Paing, J. Shin, R. Zane, and Z. Popovic, "Resistor Emulation Approach to Low-Power RF Energy Harvesting," *Power Electronics, IEEE Transactions on*, vol. 23, pp. 1494-1501.

[33] T. Esram and P. L. Chapman, "Comparison of photovoltaic array maximum power point tracking techniques," *IEEE Transactions on Energy Conversion*, vol. 22, pp. 439-449, June 2007.

[34] W. Jester and Y. Kallinderis, "Numerical study of incompressible flow about fixed cylinder pairs," *journal of Fluids and Structures*, vol. 17, pp. 561-577, 2003.